



Proportional Flexibility Matrices Using Modal Parameters Estimated with Operational Modal Analysis

Manuel Aenlle¹, Natalia García Fernández², Pelayo Fernández³

^{1,2,3} Department of Construction and Manufacturing Engineering, University of Oviedo, Spain. aenlle@uniovi.es

ABSTRACT

Several damage detection and localization techniques proposed in the literature are based changes in the flexibility matrix, which can be constructed using natural frequencies and mass-normalized mode shapes from both the un-perturbed and the perturbed system. However, in operational modal analysis (OMA), the forces are unknown, and the modal masses cannot be estimated, i.e., only the un-scaled mode shapes can be identified for each mode. In order to overcome this inconvenience, proportional flexibility matrices can also be used for damage detection without loss of accuracy. In this paper, a technique is proposed to estimate the linear relationship that exists between the modal masses of the different modes, allowing the construction of a proportional flexibility matrix.

Keywords: Flexibility matrix, Proportional flexibility matrix, modal mass, mode shapes

1. INTRODUCTION

In structural dynamics, a reduction of stiffness is commonly attributed to damage in the structure. Thus, many damage detection and localization techniques [1,2,3] are based on changes in the flexibility matrix $\Delta\mathbf{F}$:

$$\Delta\mathbf{F} = \mathbf{F}_B - \mathbf{F}_A \quad (1)$$

Where \mathbf{F}_B and \mathbf{F}_A denote the undamaged and damaged flexibility matrices, respectively.

In modal analysis, modal parameters are estimated from the experimental response of the structure and the matrix $\Delta\mathbf{F}$ can be constructed using modal parameters as:

$$\Delta\mathbf{F} = \sum_{p=1}^N \left(\frac{\boldsymbol{\phi}_{Bp} \boldsymbol{\phi}_{Bp}^T}{\omega_{Bp}^2} - \frac{\boldsymbol{\phi}_{Ap} \boldsymbol{\phi}_{Ap}^T}{\omega_{Ap}^2} \right) \quad (2)$$

Where $\boldsymbol{\phi}_{Bp}$ and ω_{Bp}^2 indicate the mass normalized mode shape and the natural frequency of the p-th mode of the experimental undamaged system, and $\boldsymbol{\phi}_{Ap}$ and ω_{Ap}^2 are those of the experimental damaged system.

In operational modal analysis, the mode shapes cannot be mass-normalized, i.e. only unscaled mode shapes can be obtained using modal estimation techniques. Thus, in order to use eq. (2), additional techniques must be used to estimate the modal masses needed to properly scale the mode shapes [4-10].

In this paper, a technique is presented to obtain proportional change flexibility matrices from modal parameters estimated with operational modal analysis. This technique is based on estimating the ratios between the modal masses of the different modes of the experimental model, for which a numerical model of the structure is used. The application of the technique is illustrated estimating the ratios of the modal masses of two scaled structural models tested in the lab.

2. PROPORTIONAL CHANGE FLEXIBILITY MATRIX

The un-scaled ($\boldsymbol{\psi}$) and scaled or mass normalized ($\boldsymbol{\phi}$) mode-shape vectors are related by the expression:

$$\boldsymbol{\phi} = \boldsymbol{\psi} \frac{1}{\sqrt{m}} \quad (3)$$

Where m is the modal mass, or alternatively:

$$\boldsymbol{\phi} = \boldsymbol{\psi} \alpha \quad (4)$$

Where $\alpha = \frac{1}{\sqrt{m}}$ is the scaling factor.

Substitution of eq. (3) in eq.(2) results in:

$$\Delta \mathbf{F} = \sum_{p=1}^N \left(\frac{\boldsymbol{\psi}_{Bp} \boldsymbol{\psi}_{Bp}^T}{m_{Bp} \omega_{Bp}^2} - \frac{\boldsymbol{\psi}_{Ap} \boldsymbol{\psi}_{Ap}^T}{m_{Ap} \omega_{Ap}^2} \right) \quad (5)$$

From which is inferred that the modal masses of both systems A and B must be known to construct the matrix $\Delta \mathbf{F}$. However, if there are no mass discrepancies between systems B and A, the modal mass matrices of systems B and A are related as [11,12]:

$$\mathbf{m}_A \cong \mathbf{T}_{\boldsymbol{\psi}}^T \mathbf{m}_B \mathbf{T}_{\boldsymbol{\psi}} \quad (6)$$

Where \mathbf{m}_A and \mathbf{m}_B are diagonal matrices containing the modal masses of system A and B, respectively, and $\mathbf{T}_{\boldsymbol{\psi}}$ is a transformation matrix which relates the modal matrices of both systems. An estimation of this matrix can be obtained with the expression [11,12]:

$$\mathbf{T}_{\boldsymbol{\psi}} = \boldsymbol{\psi}_B^+ \boldsymbol{\psi}_A \quad (7)$$

Where superindex '+' indicates pseudoinverse.

Eq. (6) demonstrates that the modal masses of system A can be estimated if the modal masses of system B are known, because the matrix $\mathbf{T}_{\boldsymbol{\psi}}$ can be obtained from the experimental modal matrices.

The modal masses of systems A and B only coincide if the matrix $\mathbf{T}_{\boldsymbol{\psi}}$ is an identity matrix. In fact, the p-th modal mass of system A is given by:

$$m_{Ap} = \mathbf{t}_{\psi p}^T \mathbf{m}_B \mathbf{t}_{\psi p} \quad (8)$$

Where $\mathbf{t}_{\psi p}$ indicates the p-th column-vector of matrix \mathbf{T}_ψ , meaning that m_{Ap} is obtained as a linear combination of the modal masses of system B.

From eq. (8) it is inferred that, in order to construct a proportional change flexibility matrix, the ratio between the modal masses of system B must be known. If we use mode 's' as reference, the matrix \mathbf{m}_B can be expressed as:

$$\mathbf{m}_B = m_{Bs} \mathbf{Z} \quad (9)$$

Where m_{Bs} is the modal mass of a mode used as reference, and \mathbf{Z} is a diagonal matrix:

$$\mathbf{Z} = \begin{bmatrix} \beta_{1/s} & 0 & \dots & 0 \\ 0 & \beta_{2/s} & \dots & 0 \\ \dots & \dots & \dots & 0 \\ 0 & 0 & 0 & \beta_{p/s} \end{bmatrix} \quad (10)$$

Which contains the ratios between modal masses:

$$\beta_{1/s} = \frac{m_{B1}}{m_{Bs}} \quad \beta_{2/s} = \frac{m_{B2}}{m_{Bs}} \quad \dots \quad (11)$$

If eq. (9) is substituted in eq. (8), the latter becomes:

$$\frac{m_{Ap}}{m_{Bs}} = \mathbf{t}_{\psi p}^T \mathbf{Z} \mathbf{t}_{\psi p} \quad (12)$$

Finally, substitution of eqs. (9) and (12) in eq. (5) gives:

$$\Delta \mathbf{F} = \frac{1}{m_{Bs}} \sum_{p=1}^N \left(\frac{\boldsymbol{\psi}_{Bp} \boldsymbol{\psi}_{Bp}^T}{\omega_{Bp}^2} - \frac{\boldsymbol{\psi}_{Ap} \boldsymbol{\psi}_{Ap}^T}{\mathbf{t}_{\psi p}^T \mathbf{Z} \mathbf{t}_{\psi p} \omega_{Ap}^2} \right) \quad (13)$$

And the proportional change flexibility matrix $\Delta \mathbf{F}_{\text{prop}} = m_{Bs} \Delta \mathbf{F}$ is expressed, in terms of modal parameters, as:

$$\Delta \mathbf{F}_{\text{prop}} = \sum_{p=1}^N \left(\frac{\boldsymbol{\psi}_{Bp} \boldsymbol{\psi}_{Bp}^T}{\omega_{Bp}^2} - \frac{\boldsymbol{\psi}_{Ap} \boldsymbol{\psi}_{Ap}^T}{\mathbf{t}_{\psi p}^T \mathbf{Z} \mathbf{t}_{\psi p} \omega_{Ap}^2} \right) \quad (14)$$

3. MODAL MASS RATIOS

Several techniques have been proposed in the literature to estimate the modal masses in operational modal analysis based on modifying the dynamic behaviour of a structure [6,9,10]. However, this approach is difficult to apply in large structures because heavy masses must be used, and also because sometimes the masses have to be attached in hard-to reach places.

In this paper, two techniques are proposed to estimate an approximate matrix \mathbf{Z} , which uses information from a numerical model.

The first technique consists of assuming that the ratio between modal masses in the experimental model is the same than that exhibited by the numerical model, i.e. if we consider modes 1 and 2, the ratio $\beta_{1/2}$ is given by:

$$\beta_{1/2} = \frac{m_{B1}}{m_{B2}} \approx \frac{m_{FE1}}{m_{FE2}} \quad (15)$$

In this case, the same modal scaling technique must be used in both the numerical and the experimental models.

The second technique combines information (mode shapes) of both the numerical and the experimental model [7,8]. With this technique, the transformation matrix \mathbf{T} [11,12] is estimated by:

$$\mathbf{T} = \boldsymbol{\Phi}_{FE}^+ \boldsymbol{\Psi}_B \quad (16)$$

Where $\boldsymbol{\Phi}_{FE}$ is the numerical mass normalized modal matrix and $\boldsymbol{\Psi}_B$ the unscaled experimental modal matrix. An estimation of the modal mass matrix of system B can be obtained with the expression [7,8]:

$$\mathbf{m}_B \cong \mathbf{T}^T \mathbf{T} \quad (17)$$

Eq. (17) only applies when the numerical mode shapes are mass normalized [7,8].

In the derivation of expression (17) it is assumed that the discrepancies between the experimental and the numerical models, in terms of mass, are small [7,8]. However, information about the numerical-experimental correlation in terms of mass can be inferred from the values of the off-diagonal terms of the inner product $\mathbf{T}^T \mathbf{T}$ [12].

4. EXAMPLES OF APPLICATION

4.1. A steel cantilever beam

Operational modal testing was performed on a steel cantilever beam structure 1.75 m long and with a rectangular hollow section 100 × 40 × 4 mm, to determine the modal parameters with respect to the weak axis.

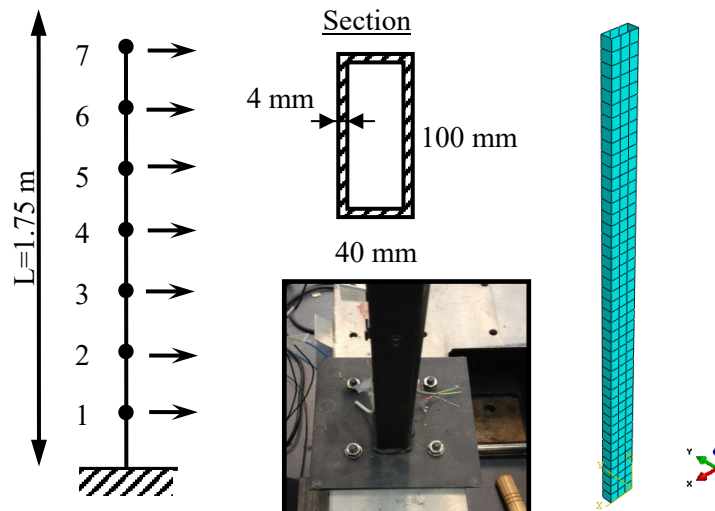


Figure 1. Geometry of the steel cantilever beam and mesh of the finite element model.

The responses were recorded in 7 DOF's during approximately 3 minutes with a sampling frequency of 2000 Hz, using 7 accelerometers with a sensitivity of 100 mV/g, located as is shown in Figure 1.

The structure was artificially excited applying repetitive hits random in time and space [13]. The modal parameters in OMA were identified with the Frequency Domain Decomposition (FDD) method [14], and the results are shown in table 1.

Table 1. Natural frequencies for the cantilever beam.

Mode	Natural frequencies (Hz)		
	OMA	FEM clamped	FEM Rot. spring
1	12.45	15.27	12.77
2	79.6	95.69	80.98
3	222.7	267.96	227.23
4	424.3	525.20	443.09

The modal masses of the structure were estimated using the mass change method [6,9,10]. The perturbation was performed attaching lumped masses of 145 grams in seven points (the same location as the sensors) with a total mass of 1015 grams, which represents 6.6% of the total mass of the beam. Thus, the mass change was proportional to the mass of the structure. The modal masses corresponding to the first four modes, with mode shapes normalized to the largest component equal to unity, are shown in Table 2.

A finite element model was also assembled in ABAQUS [15] using quadratic hexahedral elements of type C3D20R. A clamp support was considered at the bottom of the beam. The numerical natural frequencies corresponding to the first four modes are presented in table 1. It can be observed that significant discrepancies exist between the numerical and the experimental model. In order to improve the correlation, a rotational spring was introduced at the support. The natural frequencies of the updated model are also shown in Table 1, and the modal masses in Table 2.

From table 2 is inferred that the maximum error in modal mass ratios obtained with eq. (17) is approximately 12%, when compared with the modal masses obtained with the mass change method. A similar error is obtained when the ratios are obtained from the finite element model. Although it might seem that this error is large, it is of the same order as that obtained when using the mass change method.

Table 2. Modal masses and ratios for the cantilever beam. Mode shapes normalized to the largest component equal to unity.

Mode	$T^T T$		OMA		FEM 1 Clamped		FEM 2 rotational spring		Error (%)	
	Modal mass	Ratio	Modal mass	Ratio	Modal mass	Ratio	Modal mass	Ratio	OMA $T^T T$	OMA FEM2
1	4.10	1.000	3.9556	1.0000	3.67	1.000	4.04	1.000	-	-
2	4.07	0.994	3.8842	0.9820	3.71	1.000	4.00	1.004	1.22	2.24
3	4.16	1.016	4.0911	1.0343	3.71	1.000	4.02	1.003	1.77	3.03
4	4.25	1.037	4.6468	1.1747	3.62	0.999	4.06	0.997	11.72	15.13

4.2. A T steel structure

This structure consists of a vertical steel column (height 1.70 m) with a rectangular hollow steel section $8\text{cm} \times 4\text{cm}$ and thickness 4mm , and a horizontal wooden beam (length 2 m) with rectangular section $12.7\text{cm} \times 7\text{cm}$ (see Fig. 5). The structure is fixed at the bottom of the column, and a steel plate was welded at the top of the column in order to connect it to the wooden beam using four bolts. The total mass of the steel part was 11.96 kg and that of the wooden part 11.46 kg .

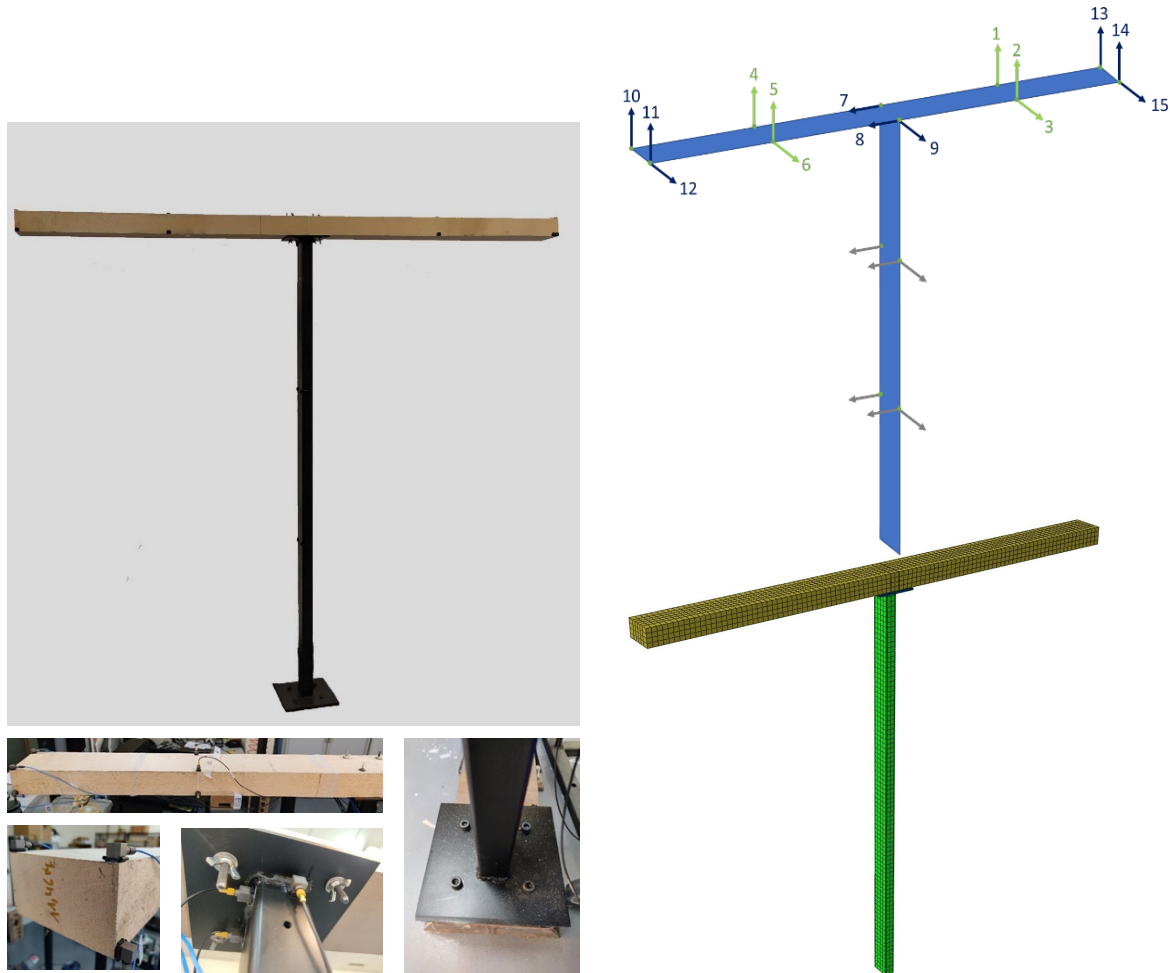


Figure 2. Geometry of the T structure, test setup and finite element model.

A finite element model was assembled in ABAQUS [15] using the geometrical parameters described in the previous paragraph and meshed with 3D elements (20 nodes with reduced integration). The following mechanical properties were considered for steel: mass density $\rho = 7850\text{ kg/m}^3$, Young's modulus $E = 210 \cdot 10^9\text{ N/m}^2$ and Poisson ratio $\nu = 0.3$, and wood: mass density $\rho = 644\text{ kg/m}^3$, Young's modulus $E = 13.5 \cdot 10^9\text{ N/m}^2$ and Poisson ratio $\nu = 0.38$. The numerical natural frequencies corresponding to the first 8 modes are shown in table 3, whereas the mode shapes are presented in Fig. 3.

The experimental modal parameters were estimated with experimental and operational Modal Analysis (OMA). In OMA, the responses were recorded for approximately 4 minutes with a sampling frequency of 1632 Hz using two data sets (Fig. 2). The responses were measured in twenty-one points using 15 accelerometers (100 mV/g), and the modal parameters were estimated with the stochastic subspace iteration (SSI) [14].

The modal parameters were also estimated with experimental modal analysis (EMA) using the Complex Mode Indicator Function CMIF technique [13,17,18]. Same sensors, instrumentation, and test setup as

those used in OMA were used in the EMA, being the structure excited with an impact hammer applying the forces in DOF's 9, 14 and 15, respectively. The natural frequencies estimated with EMA and OMA, corresponding to first eight modes, are shown in table 3.

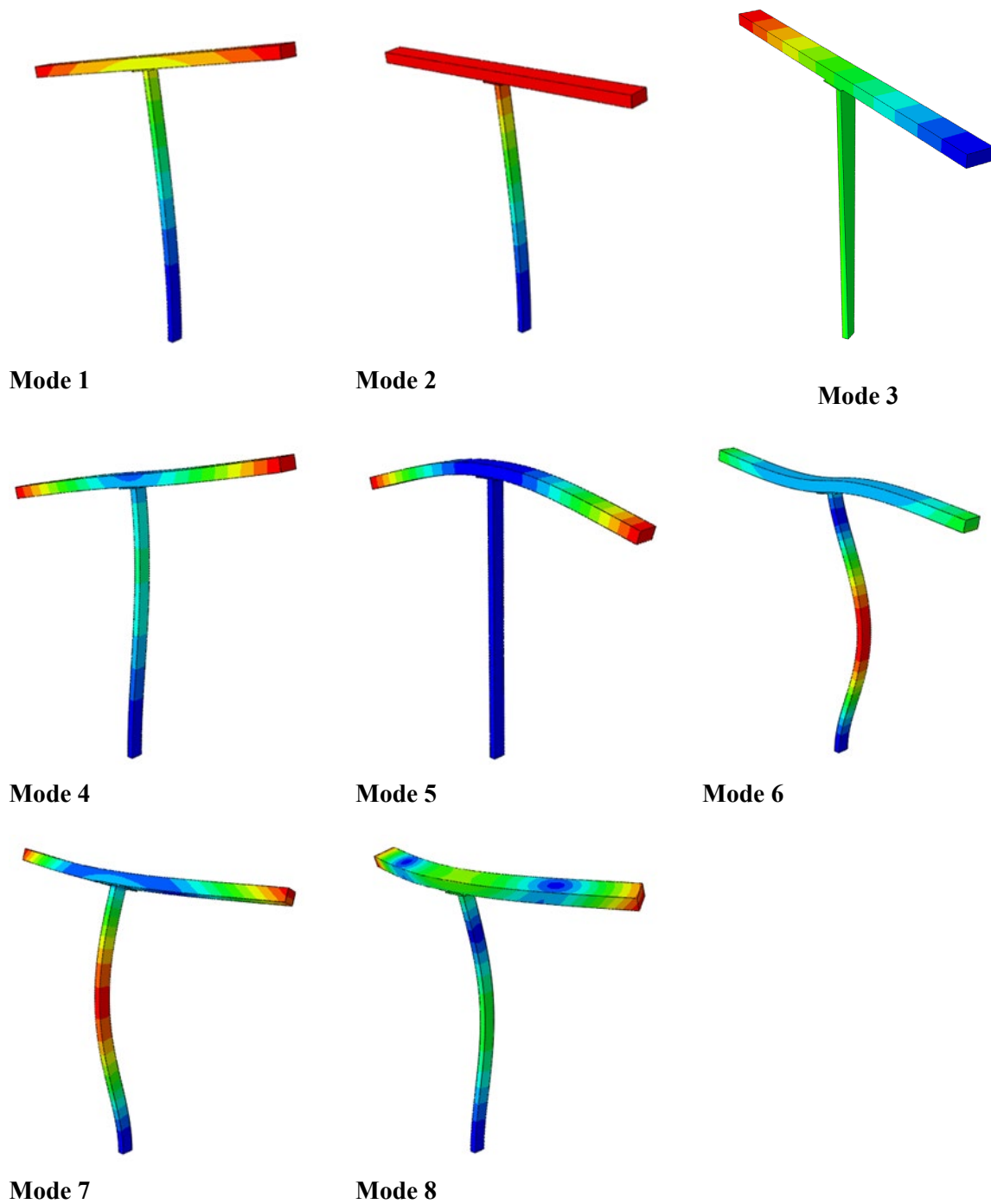


Figure 3. Geometry of the T structure, test setup and finite element model.

Table 3. Natural frequencies of the T structure.

Mode	Frequency (Hz)		
	FE model	OMA (SSI)	EMA
1	6.21	5.28	5.31
2	11.89	10.34	10.39
3	13.07	12.07	11.79
4	24.69	18.88	18.37
5	56.07	50.27	50.75
6	95.45	76.82	75.26
7	110.48	99.97	100.31
8	151.47	138.73	140.38

The modal masses estimated with EMA, together with those extracted from the finite element models and those estimated using Eq. (17), are shown in Table 4, where the mode shapes have been normalized to the largest component equal to unity. The ratios between modal masses, using the first mode as reference, are shown in Table 4.

Table 4. Modal masses and ratios for the T structure.

Mode	$T^T T$		EMA		FEM	
	Modal mass	Ratio	Modal mass	Ratio	Modal mass	Ratio
1	19.23	1.0000	18.90	1.0000	19.58	1.0000
2	15.38	0.80	12.87	0.68	15.47	0.79
3	3.78	0.20	3.70	0.20	3.82	0.19
4	4.41	0.23	4.333	0.23	4.62	0.24
5	2.53	0.13	2.79	0.15	2.77	0.14
6	8.31	0.43	8.75	0.46	9.54	0.49
7	8.60	0.45	8.16	0.43	8.50	0.43
8	3.90	0.20	3.77	0.20	3.98	0.20

It is inferred from table 4 that the maximum error in modal mass ratios, obtained with eq. (17), is approximately 17% for the second mode, whereas a better accuracy has been achieved for the rest of the modes. Although it might seem that the error is large, it must be emphasized that the modal mass is the least reliable parameter when experimental analysis (EMA) is used, and similar or larger errors can be obtained with EMA.

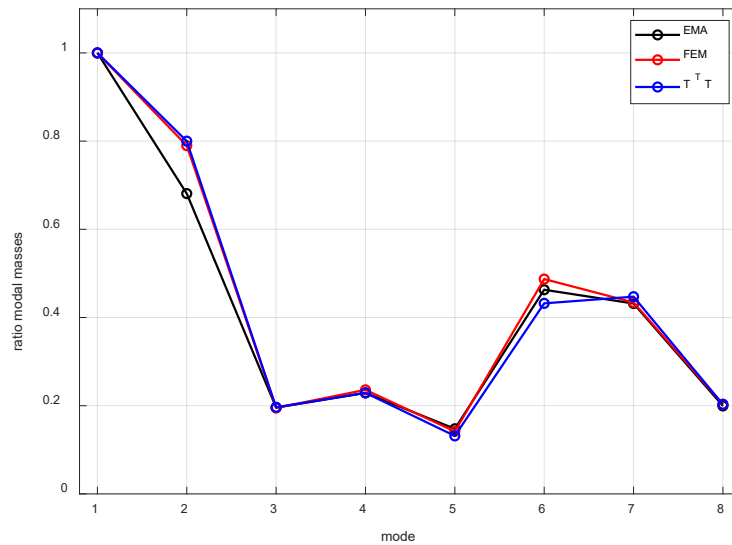


Figure 4. Ratio between modal masses for the T structure. Mode shapes normalized to the largest component equal to unity.

5. CONCLUSIONS

- A technique to construct a proportional flexibility matrix for damage detection and localization is proposed. A numerical model is used to estimate the ratio between the modal masses of the undamaged system.
- Two different methods have been proposed. The first one consists of assuming that the ratio between modal masses in the experimental model is the same than that exhibited by the numerical model. The second technique combines information (mode shapes) of both the numerical and the experimental model to estimate the transformation matrix \mathbf{T} , and the modal masses are estimated with the inner product $\mathbf{T}^T \mathbf{T}$.
- The technique has been validated by estimating the modal mass ratios of two scaled structural models tested in the lab: a steel cantilever beam and a steel-wood T-structure. Errors of similar magnitude to those obtained with EMA and the mass change method have been observed.

ACKNOWLEDGEMENTS

This work was supported by the Spanish State Research Agency through the grant PID2023-147535OB-100 funded by MICIU/AEI/10.13039/501100011033 and FEDER, EU, grant MICIU-20-PID2019-105593GB-100 funded by MICIU/AEI/10.13039/501100011033, and grant MICIU-21-PRE2020-094923 funded by MICIU/AEI /10.13039/501100011033 and FSE+.

REFERENCES

- [1] E. Reynders, G. Roeck. A local flexibility method for vibration-based damage localization and quantification. *Journal of Sound and Vibration*. 329 (12),2367-2383, 2010.
- [2] G. Bernagozzi, S. Mukhopadhyay, R. Betti, L. Landi, P.P. Diotallevi. Proportional flexibility-based damage detection for buildings in unknown mass scenarios: The case of severely truncated modal spaces. *Engineering Structures*, 259 (15), 114145, 2022.

- [3] D. Bernal. Load Vectors for Damage Localization. *Journal of Engineering Mechanics*, 128 (1), 2002.
- [4] M. Aenlle, R. Brincker, M. Juul. Modal Mass and Length of Mode Shapes in Structural Dynamics. *Shock and Vibration*, 8648769, 2020.
- [5] M. Aenlle, R. Brincker. Basic Concepts of Modal Scaling. *Proceedings of the 8th International Operational Modal Analysis Conference*, Copenhagen, Denmark, 2019.
- [6] M. Aenlle, R. Brincker, F. Pelayo, A. Fernández-Canteli. On exact and approximated formulation for scaling-mode shapes in operational model analysis by mass and stiffness change. *Journal of sound and vibration*, 331, 622–637, 2012.
- [7] M. Aenlle, R. Brincker. Modal Scaling in Operational Modal Analysis using a Finite Element Model. *International Journal of Mechanical Sciences*, 76, 86-101, 2013.
- [8] M. Aenlle, R. Brincker. Modal Scaling in OMA Using the Mass Matrix of a Finite Element Model. *Proceedings of the International Modal Analysis Conference (IMAC) XXXII*, Orlando, USA, 2014.
- [9] D. Bernal. Modal Scaling from Known Mass Perturbations. *Journal of Engineering Mechanics*, 130, 1083-1088, 2004.
- [10] M. Aenlle, P. Fernández, R. Brincker, A. Fernández-Canteli. Scaling Factor Estimation Using an Optimized Mass Change Strategy, *Mechanical Systems and Signal Processing*, 24, 3061-3074, 2010.
- [11] R. Brincker, A. Skafte, M. Aenlle, A. Sestieri, W. D’Ambrogio, A. Fernández-Canteli. A local correspondence principle for mode shapes in structural dynamics. *Mechanical Systems and Signal Processing*. 45, 91-104, 2014.
- [12] M. Aenlle, N. García Fernández, P. Fernández. Rotation of mode shapes in structural dynamics due to mass and stiffness perturbations, *Mechanical Systems and Signal Processing*, 212, 111269, 2024.
- [13] P. Fernández, M. Aenlle, R. Brincker, A. Fernández-Canteli. Artificial Excitation in Operational Modal Analysis. *Proceedings of the 3rd International Operational Modal Analysis Conference*, Ancona, Italy, 2009
- [14] R. Brincker, C. Ventura. *Introduction to Operational Modal Analysis*. Chichester: John Wiley & Sons Ltd, 2015.
- [15] ABAQUS, Finite Element Analysis Software, Dassault Systemes, Velizy-Villacoublay, France.
- [16] D.J. Ewins. *Modal Testing: Theory, Practice and Application*, Second Ed. London: Research Studies Press LTD, 2000.
- [17] N.M.M. Maia, J.M. Montalvao e Silva. *Theoretical and Experimental Modal Analysis*. England: Research Studies Press LTD. 2003.
- [18] W. Heylen, S. Lammens, P. Sas. *Modal Analysis theory and testing*. Belgium: Katholieke Universiteit Leuven, Faculty of Engineering, 2007.